A quantitative method to compare the effect of thermal aging on the mechanical performance of fire protective fabrics

Patricia I. Dolez[a,b]*, Namrata S. Tomer[b], Yassine Malajati[b]

[a]*Department of Human Ecology, University of Alberta, Edmonton, AB, Canada*

[b]*Department of Mechanical Engineering, Ecole de technologie superieure, Montreal, QC, Canada*

* Corresponding author: pdolez@ualberta.ca

Abstract

A method has been proposed to provide a means to compare in a quantitative and comprehensive way the mechanical performance of fire protective fabrics under long-term thermal exposure. These high-performance materials experience a reduction in their performance over time due to the various conditions they are exposed to during the lifetime of the clothing. The proposed method consists in a system of two equations fitting the time-temperature-performance data: the Arrhenius model combined with the time-temperature superposition principle, and the 3-parameter Hill equation. The result of the data analysis using this method is provided in terms of four parameters: the temperature effect, the time rate, the degradation midpoint time, and the ultimate strength. It was used to compare the effect of accelerated thermal aging on the tear strength of seven different fabrics used in fire protective clothing. In all cases, a very good agreement was observed with both the Arrhenius model and the Hill equation. However, none of the fabrics studied appeared to stand as displaying all the characteristics that would be ideal for long-term fire protection. The best solution is thus a compromise that will depend on the type of activity conducted and the type of conditions experienced.

Keywords: Fire protective fabrics; thermal aging; tear strength; Arrhenius model; Hill equation

1. Introduction

The performance of the materials used to make firefighters' bunker suits, as well as protective clothing and equipment for workers in industries at high risk of heat and flame exposure such as oil and gas industry, is critical for ensuring the safety of those wearing them. Indeed, burns may not be as prevalent as other causes of injury and fatality such as sudden cardiac arrest and internal trauma in the case of death and musculoskeletal strain and sprain in the case of injury e.g. for firefighters[1,2]. Yet, they are among the worst in terms of psychological impact and lifelong consequences on the appearance of injured victims[3].

For that purpose, advanced materials have been developed over the last fifty years to manufacture high performance fire protective clothing. Some of these fibers are inherently flame resistant and display higher mechanical properties and improved chemical and thermal resistance. Table 1 provides a list of fibers most often used in fire protective fabrics along with relevant properties.

Table 1. List of high performance fibers used in fire protective fabrics, with relevant characteristics

Name	Trade name	Decomposition temperature in air (°C)	Thermal index (°C)	Strength (GPa)	References
Poly(para-phenylene terephthalamide)	Kevlar®, Twaron®	425	190	2.8-4.1	4,5
Poly(meta-phenylene isophthalamide)	Nomex®, Conex®	450	200	0.5-0.7	5,6
Melamine	Basofil®	370	200	0.03-0.06	5,7
Polybenzimidazole	PBI	580	250	0.35	5,7
polybenzoxazole (PBO)	Zylon®	600	310	5.8	5,8

However, if these fibers exhibit exceptional performance when new, their properties may be affected in the long term as a result of the conditions encountered in service. As a matter of fact, a series of testing campaigns performed on used firefighter turnout gear, some retired and some not, have revealed significant losses of some properties[9-12]. For instance, 65% of the less than 4 year-old garments tested did not meet the relevant National Fire Protection Association (NFPA) water penetration requirements[13]. That value increased to 67% for garments aged 5 to 10 years, and to 81% for garments aged 10 to 12 years. Mechanical performance, including tensile strength, seam strength, and tear strength, was also an issue. For example, close to 10% of the outer shell samples tested in the less than 4-year-old category did not meet the relevant NFPA requirements. In the particular case of PBO, its use has been excluded from ballistic protective clothing because of major losses in mechanical strength observed as a result of exposure to moisture[14].

Indeed, studies involving accelerated aging have shown that the high-performance materials used to manufacture fire protective clothing are sensitive to the environmental agents to which the clothing is exposed in service[15]. This includes heat, UV, moisture, abrasion, and laundering. In particular, exposure to elevated temperatures has been shown to induce large decreases in the mechanical performance of yarns and fabrics. For instance, a 50% reduction in tensile strength of a 60/40 wt% Kevlar®/PBI spun yarn and Kevlar®/PBI spun yarn / Kevlar® filament twill weave fabric was recorded after 300 hours of exposure at 190°C in an air-circulating oven, which is the maximum continuous operating temperature of Kevlar® in air[16]. This was attributed to an increase in the crystallite size in the direction parallel to the coplanar sheets occurring simultaneously with a disruption of the crystalline lattice in the perpendicular direction in the case of Kevlar®, and random chain scissions in the case of PBI[17].

The thermal aging of Nomex® fibers has also been shown to lead to a reduction in the fiber elastic modulus, tensile strength, and elongation at break[18]. Fibers held at 200°C, which is the maximum continuous operating temperature of Nomex® in air, showed a gradual decrease in crystallinity with increasing exposure time; they eventually reached a state of zero crystallinity after 1750h of exposure at 200°C. In the case of melamine fibers, thermal aging at 150°C for 7 days induced an increase in the crystallinity along with a change in the crystalline structure of the material and an increase in the crystallite size[19]. Finally, when aged for 2500h at 205°C, which is far below their maximum continuous operating temperature of 310°C, PBO fibers experienced a 40% reduction in tensile strength[20]. By comparison, the reduction in tensile strength of Kevlar® fibers aged in the same conditions was 60%.

A few studies have compared the behavior of fabrics made of the different types of fire resistant, high performance fibers. For instance, Ozgen and Pamuk tested the tensile strength of woven fabrics produced using 100% Kevlar®, 100% Nomex®, and 50/50 Kevlar®/Nomex® yarns that were aged at 220 and 300°C for times up to 30 days[21]; they reported that the highest loss in strength was measured for the 100% Kevlar® fabrics. For their part, Rossi et al. subjected samples of fabric assemblies consisting of different outer shell materials, moisture barriers, and thermal liners typical of what is used in firefighters' protective suits to either radiant or convective heat[22]. Even if comparisons were limited by the fact that they used different exposure times for the different fabrics, they reported differences in the effect produced on tensile and tear strength between the different types of materials.

These data show the importance of considering the effect of the thermal conditions that will be experienced by the clothing when designing or selecting fire protective gear. In addition, comparing the thermal aging behavior of different protective fabrics over the whole aging process is of great interest. In particular, quantifying the individual contribution of temperature and time on the performance loss can provide valuable information to allow matching the fabric performance with the specificities of the clothing use conditions. For instance, protective clothing used in front line activities will be exposed to higher levels of heat compared to support positions.

A data analysis procedure is proposed here for that purpose. It consists of a system of two equations fitting the time-temperature-performance data. The results are provided in terms of four parameters quantifying individually the temperature effect, the time rate, the degradation midpoint time, and the ultimate strength. This data analysis method was used to compare the effect of accelerated thermal aging on the tear strength of seven different fabrics used in fire protective clothing, which has never been reported before.

2. Materials and Methods

Seven commercially available fabrics typically used in fire protective clothing have been selected for the study. They correspond to various ratios of different types of fire resistant, high-performance fibers. Table 1 provides the composition and structure of these fabrics. They had a similar mass per surface area of 255 g/m^2.

Table 2. Composition and structure of the seven fabrics included in the study.

Fabric	Composition	Structure
# 1	100% Kevlar® spun yarns	Plain weave
# 2	93% Nomex®, 5% Kevlar®, 1% carbon (Nomex® IIIA) spun yarns	Plain weave
# 3	60% Kevlar®/40% Nomex® IIIA spun yarns	Rip Stop
# 4	60% Kevlar®/20% Nomex®/20% PBO spun yarns	Rip Stop
# 5	60% Kevlar®/40% Basofil® spun yarns	Rip Stop
# 6	100% Nomex® spun yarns	Plain weave
# 7	60% para-aramid/40% PBI spun yarns/Kevlar® filament	Twill with Kevlar® filament network

Fabric specimens were subjected to accelerated thermal aging using an electrical convection oven where they were left in a hanging position for durations between 1 and 500 hours. Five values of temperature were selected for the accelerated aging campaign: 150, 190, 210, 235, and 300°C. This choice was based on the thermal index of the different types of fibers, which ranges from 190°C for Kevlar® to 310°C for PBO[5]. The selection of the aging temperature values also took into account the exposure conditions typically faced by fire fighters[23]: up to 60°C and/or 1.4 kW/m^2 for routine conditions, within the range 60-300°C and/or 1.4-10 kW/m^2 for hazardous conditions, and above 300°C and/or 10 kW/m^2 for emergency conditions.

The effect of accelerated thermal aging on the fabrics was assessed on terms of tear strength. The test method used was similar to ASTM D5587 except that the size of the specimens was reduced due to the finite amount of fabric available. Trapezoidal tear specimens with dimensions of 50.8 x 101.6 mm were cut in the fabric weft direction according to the schematic representation in Fig. 1. They included a 10.6 mm long notch in the trapezoid small base. The

specimens were fixed in the grips of an Alliance 2000 (MTS) universal testing machine by clamping them along the legs of the trapezoid shape, leaving the long base opposite to the notch wavy. The grips were pulled apart at a rate of 200 mm/min until the specimen was completely torn apart. Four specimens were tested for each condition. The tear strength was computed as the average of the maximum force values measured for each specimen.

Complementary thermogravimetric analysis (TGA) was performed using a Pyris Diamond (Perkin Elmer) to determine the thermal stability of the fabrics. The measurement was conducted between 30°C and 1000°C at 20°C/min under nitrogen atmosphere. The weight of the samples was in the range of 5-10 mg.

Fourier-transform infrared (FTIR) analysis was also carried out using a Thermal Continuum FTIR (Nicolet) microscope. Individual fibers were pulled from the fabric, crushed and flattened with a small roller and then taped onto an aluminum-coated slide. Germanium crystal was used for the analysis and a total of 120 scans with a resolution of 8 cm^{-1} were carried for each spectrum.

Finally, the effect of thermal aging on the fabric microstructure was investigated using a scanning electron microscope (SEM) (S3600N, Hitachi). The specimens were metallized using gold sputtering before being observed.

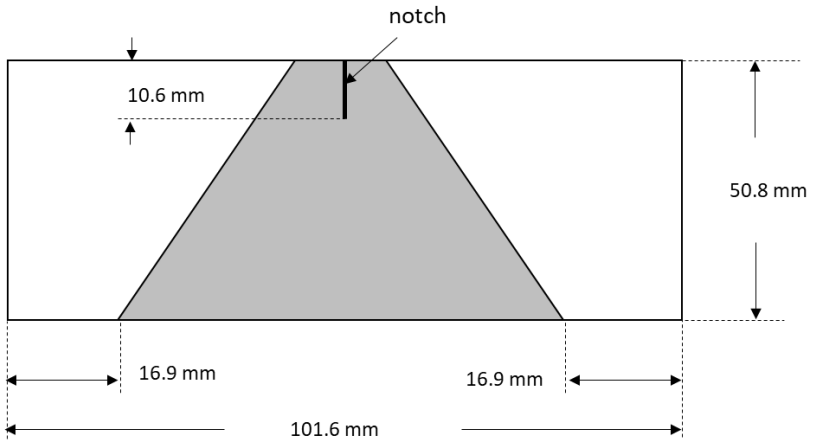

Figure 1. Geometry of the trapezoidal tear test specimen

3. Analytical approach

This section gives the step-by-step analysis that was applied to the tear strength data provided by the accelerated aging program. The rational behind the development of this data analysis technique was to extract a series of parameters defining the characteristics of the material aging behavior, in particular the effect of time and temperature, from a set of time-temperature-residual performance data resulting from an accelerated thermal aging treatment performed for different durations and at different temperatures.

One of the most commonly used methods to predict the service life of thermally aged polymers is based on the Arrhenius model[25,26]. This model is based on the assumptions that the degradation is homogeneous throughout the material, that a single chemical reaction governs the degradation process, and that the reaction rate *K* varies with the temperature according to the following equation:

$$K = K_0 \, exp\left(-\frac{E_a}{RT}\right) \qquad \text{Eq. 1}$$

E_a is the activation energy of the reaction, which represents the sensitivity of the degradation process to the temperature. R is the universal gas constant and T is the absolute temperature. This model has provided satisfactory results for high-performance fibers such as Kevlar® and PBI[16], Nomex®[24], and PBO[20] when used to describe the change in various properties resulting from thermal aging. For materials whose behavior deviates from linearity with the Arrhenius model, the Eyring model, which adds an entropic term to the enthalpy of the Arrhenius description, may be used alternatively[27].

Two strategies can be employed to analyze a set of performance-time-temperature aging data using the Arrhenius model. The first one consists in arbitrarily selecting a response value, for instance 50% of property retention, and determining the aging time corresponding to this response value at each aging temperature[25]. The Arrhenius plot representing the aging time on a logarithmic scale as a function of the reciprocal temperature is then constructed using this set of data to yield the activation energy of the degradation reaction. However, this technique only makes use of a limited number of data points.

The second strategy allows using the entire set of data points resulting from the property variation measurement by applying the time-temperature superposition (TTS) principle[26]. According to this principle, which applies to linear viscoelastic materials in the domain of interest, the time-dependant plots of the property variation at different temperatures have an identical shape when expressed as a function of the logarithm of time. A master curve is constructed by horizontally shifting the data sets corresponding to the different aging temperatures expressed on a semi-logarithmic plot onto the curve corresponding to a temperature selected as a reference (an example of the TTS master curve construction process is illustrated in Fig. 3 and 4). The shift factors thus generated may then be used to construct an Arrhenius plot.

Now, let's consider the variation of a material property as a function of time throughout the material aging process using the master curve provided by the application of the TTS principle to the performance-time-temperature data. As aging starts, the material quits its original condition after a more or less long induction period and a reduction in the measured property, for instance tensile strength, is recorded. At the other end of the aging process, the property eventually reaches a plateau corresponding to its ultimate value, which may be zero. If the material property loss is governed by a single mechanism, a one-step transition is recorded between the initial and the final condition; the curve expressing the property vs. log of time

displays a sigmoid shape. One of the most common models used to fit sigmoid curves is the 3-parameter Hill equation[28]:

$$Y = \frac{\alpha\, x^n}{x^n + K^n} \qquad \text{Eq. 2}$$

In this general form of the Hill equation, *n* corresponds to the slope of the sigmoid curve; *α* is the value of the y-axis asymptote; and *K* relates to the inflexion point. To fit the aging data master curve, the form P = 1 – Y of the Hill equation would be used, with P being the material performance under investigation. The Hill equation is largely employed in pharmacology and biology to fit concentration-response curves[29]; it has also been successfully used to model the soiling of float glass in polluted atmospheres[30] and coated fabrics[31] for instance.

In the proposed method, the effect of temperature on the aging process is thus analyzed using the Arrhenius model combined with the TTS principle. The resulting master curve at a set reference temperature is then fitted with the 3-parameter Hill equation to extract the influence of aging time on the performance studied.

4. Results

4.1 Fabric #1

The thermal behavior of Fabric # 1 as characterized by TGA is shown in Figure 2. The thermal degradation of the 100% Kevlar® fabric occured in one rapid degradation step at 575°C, which is the characteristic of decomposition of Kevlar® 29 fibers[32]. The initial slight weight loss at 100°C is attributed to the release of adsorbed moisture in agreement with the work of Shubha et al.[33]. The highest weight loss of 52% associated to an endothermic signal was observed between 550°C and 590 °C.

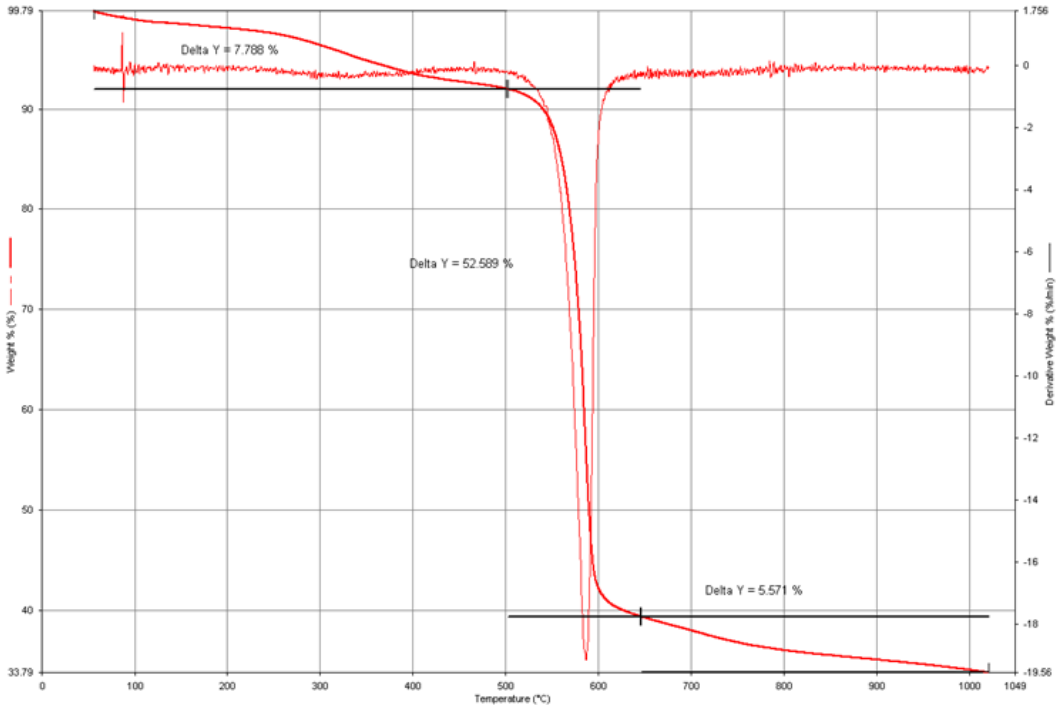

Figure 2. TGA and time derivative spectrum of Fabric # 1.

Figure 3 shows the variation of the tear strength retention as a function of aging time at different aging temperatures. At each aging temperature, a steady decrease in tear strength with aging time was observed. A decrease in tear strength was also recorded when the aging temperature was increased. The loss in tear strength reached 50% after 150 hours of aging at 150°C, even though this temperature is well below the thermal index of 190°C reported for Kevlar® from which this fabric is made[5]. After 1 hour of exposure at 210°C, the tear strength retention was 65% and 16% after the same time at 300°C.

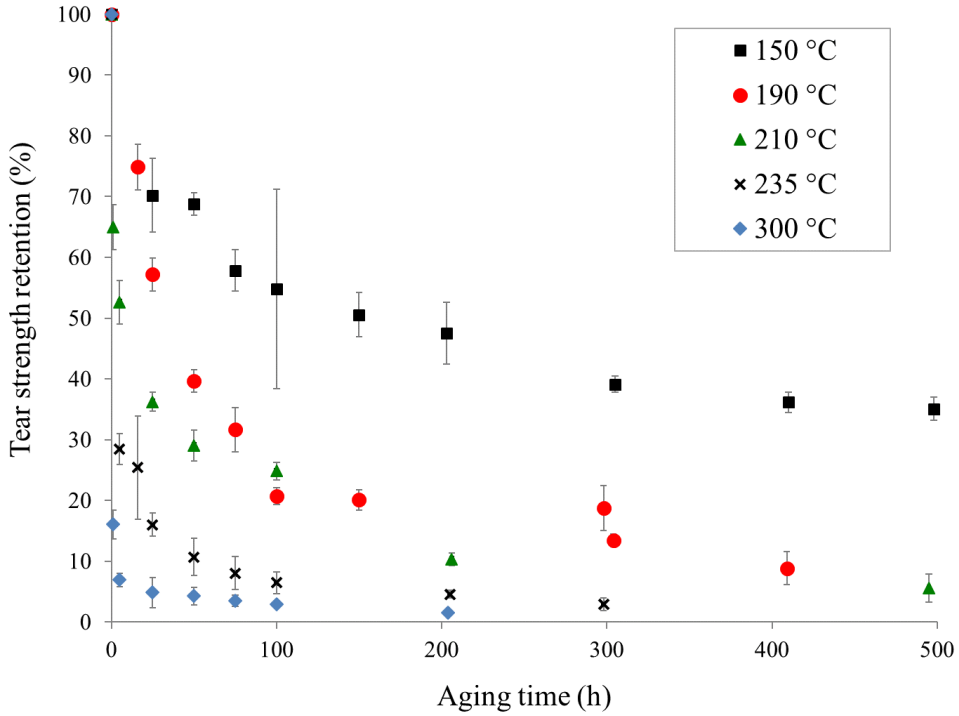

Figure 3. Variation of the tear strength retention as a function of the aging time at aging temperatures of 150, 190, 210, 235, and 300°C for Fabric # 1.

The data shown in Figure 3 were analyzed using the TTS principle described in section 3. The sets of data points corresponding to the aging temperatures of 190, 210, 235, and 300°C expressed on a semi-logarithmic scale were shifted horizontally on the 150°C set of data points until a smooth curve was achieved. The resulting master curve is shown in Figure 4.

The shift factors provided by the application of the TTS principle yielding to this master curve are displayed in an Arrhenius plot in the insert in Figure 4. A linear relationship with a R^2 value of 0.989 is observed between the logarithm of the shift factors and the reciprocal temperature, which indicates that the effect of thermal degradation on the tear strength of Kevlar® can be described satisfactorily using the Arrhenius model. The corresponding activation energy obtained is 95 kJ/mol.

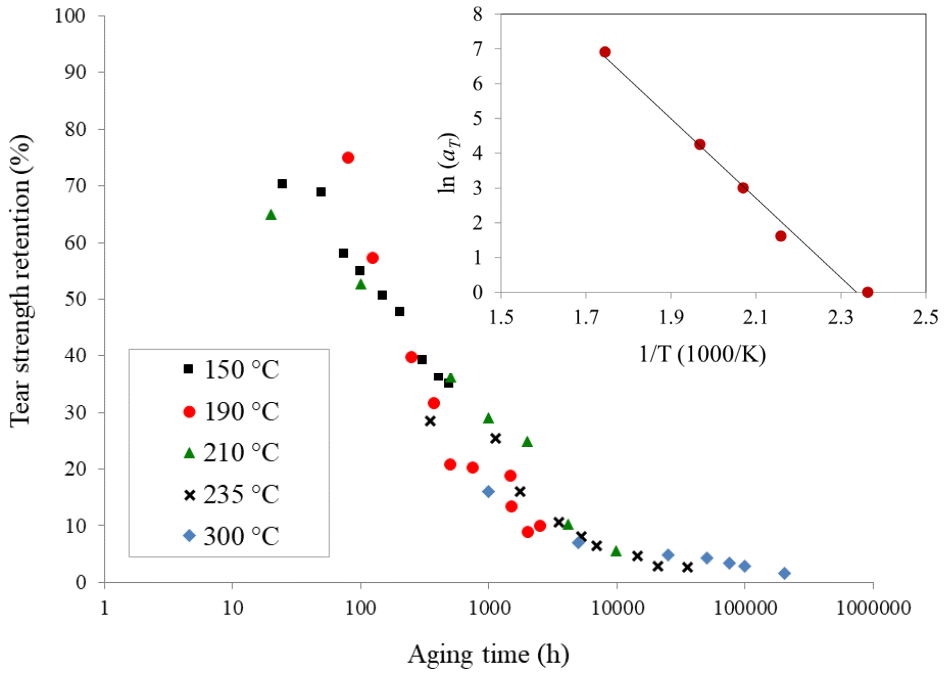

Figure 4. TTS master curve at a temperature of 150°C for Fabric # 1 (In insert: Arrhenius plot of the shift factors).

In order to get access to the time aspects of the aging behavior, the data points corresponding to the tear strength retention master curve displayed in Figure 4 were fitted with the Hill equation using a least square method. The result is shown in Figure 5. A good agreement between the data points and the model was obtained. The values of the three parameters of the Hill equation are 0.64 for the slope, 140 hours for the inflexion point, and 0 for the lower asymptote.

FTIR spectra of unaged and aged specimens were measured to investigate if the decrease in strength as a result of thermal aging was a result of oxidative chain scission of the fibers. A qualitative analysis of the spectra showed no evidence of chemical changes between the aged and unaged samples. This absence of modification in the FTIR absorption bands after thermal aging is in agreement with what has been reported for a Kevlar-PBI blend fabric (Figure 6)[16], which corresponds to Fabric #7 in this study. In their paper, the authors provide a detailed analysis of the band assignment of the absorption peaks for the unaged Kevlar-PBI yarns as well as would be expected as a result of thermal aging: absorption bands of oxidized groups, especially in the carbonyl region. It must be noted that they found no sign of peaks characteristic of PBI fibers in the spectra obtained of the unaged Kevlar-PBI yarns, which matched those of a Kevlar thread[16]. This was attributed to the higher Kevlar content in the fabric.

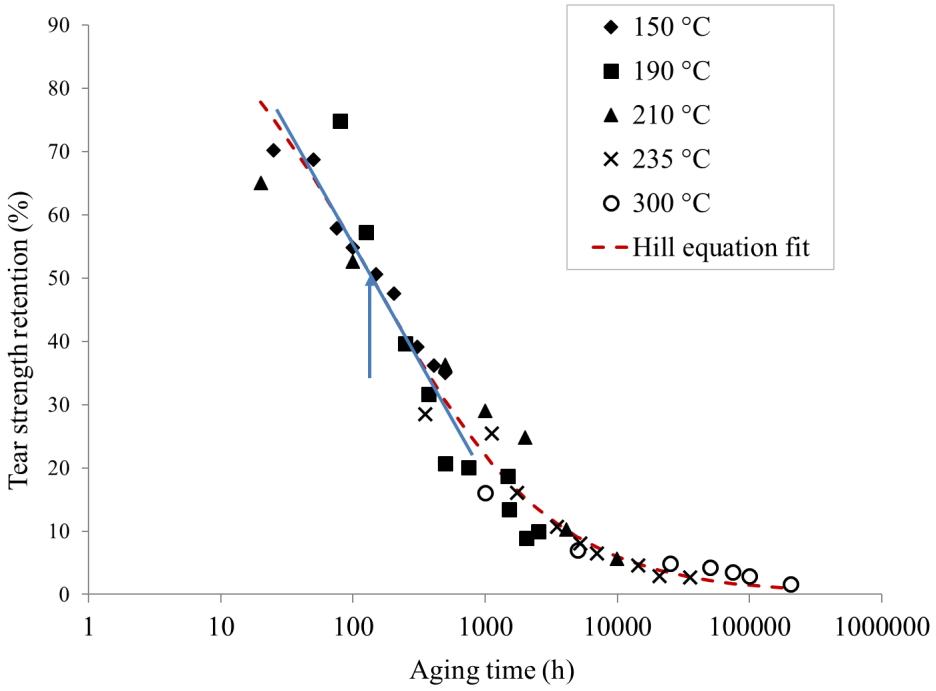

Figure 5. TTS master curve at a temperature of 150°C with the Hill equation fit for Fabric # 1 (location of and tangential line at the inflexion point of the sigmoid fit indicated).

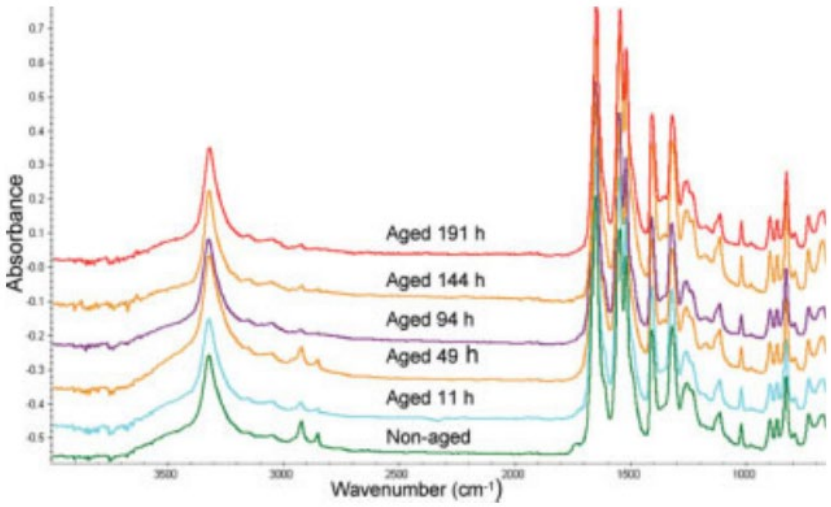

Figure 6. FTIR spectra of Kevlar/PBI yarns unaged and aged at 275°C for periods between 11 and 191h (Reproduced from Arrieta et al.[16]).

Figure 7 shows an SEM image of an unaged specimen of Fabric # 1. The fibers had diameters in the range of 15-20 µm. An observation at higher magnification showed no difference in the fiber morphology between unaged and aged conditions (Figure 8).

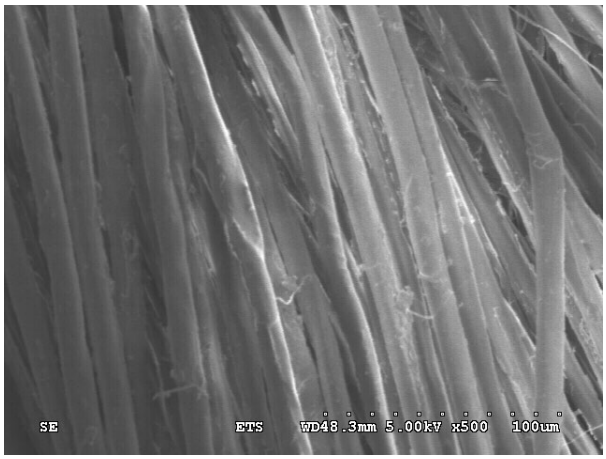

Figure 7. SEM picture of Fabric # 1, unaged (magnification x 500).

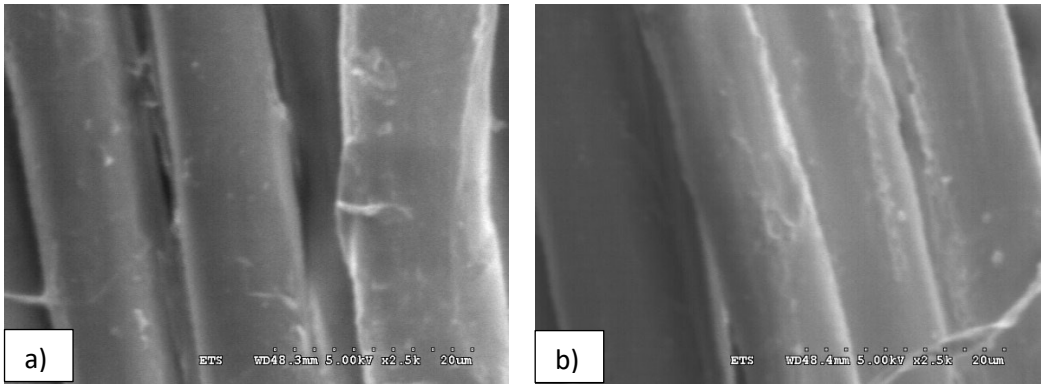

Figure 8. SEM pictures of Fabric # 1, a) unaged and b) aged at 300°C for 100 hours (magnification x 2,500).

4.2 Fabric #2

The TGA curve of Fabric # 2 (Figure 9) shows a thermal event much more complex than for Fabric # 1. This can be associated with the fact that yarns of Fabric #2 are a blend of Nomex®, Kevlar® and carbon. As for Fabric #1, an initial weight loss extending from room temperature to 100°C can be ascribed to the release of adsorbed moisture. Indeed, the presence of adsorbed moisture has also been reported in the case of Nomex® fibers[34]. From 250°C to 800°C, the weight loss took place in three steps. The largest drop in weight between 410°C and 550°C can be associated with the decomposition of Nomex®[5]. The final weight loss at 580°C corresponds to the decomposition of Kevlar®[32]. The small weight loss between 250°C and 410°C may be due the decomposition of materials used as a finish on the fabric, for instance used for water repellency[35] and/or to limit static charge build-up[36].

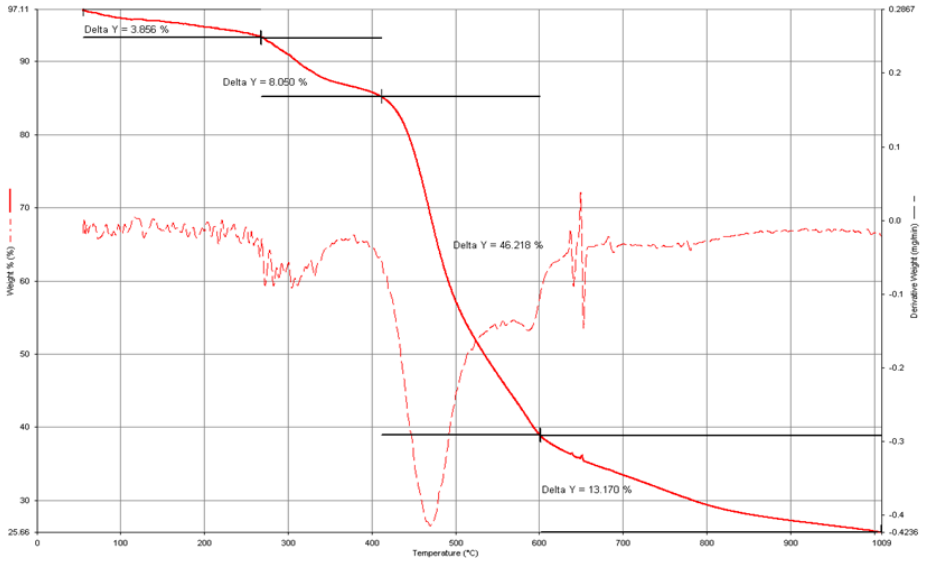

Figure 9: TGA and time derivative spectrum of Fabric #2.

Figure 10 displays the results in terms of tear strength retention as a function of the aging time for the different aging temperatures. Fabric #2 displayed better stability to aging than Fabric #1. For instance, the tear retention at 300°C was 60% after 5 hours whereas it was 7% for Fabric #1. It also offered a much better performance at 150°C and retained 70% of its strength after 500 h of exposure.

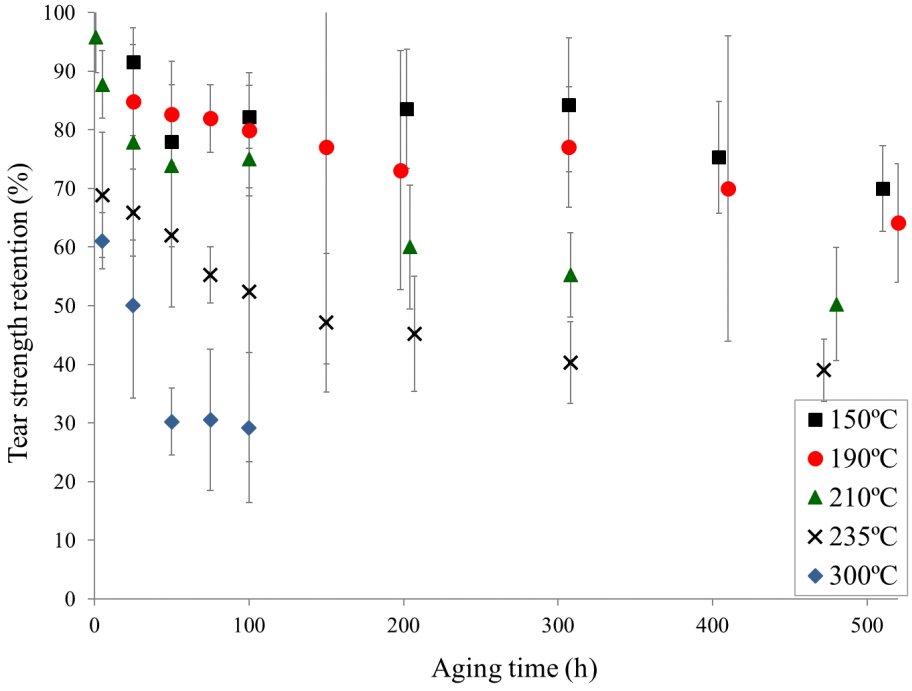

Figure 10. Variation of the tear strength retention as a function of the aging time at aging temperatures of 150, 190, 210, 235, and 300°C for Fabric # 2.

The TTS master curve for Fabric #2 using the curve at 150°C as a reference is shown in Figure 11. The Arrhenius plot created using the shift factors provided by the TTS technique is given in insert in Figure 11. Again, the Arrhenius model accommodates the data satisfactorily with a correlation coefficient of 0.984. The activation energy calculated using this approach is 90 kJ/mol.

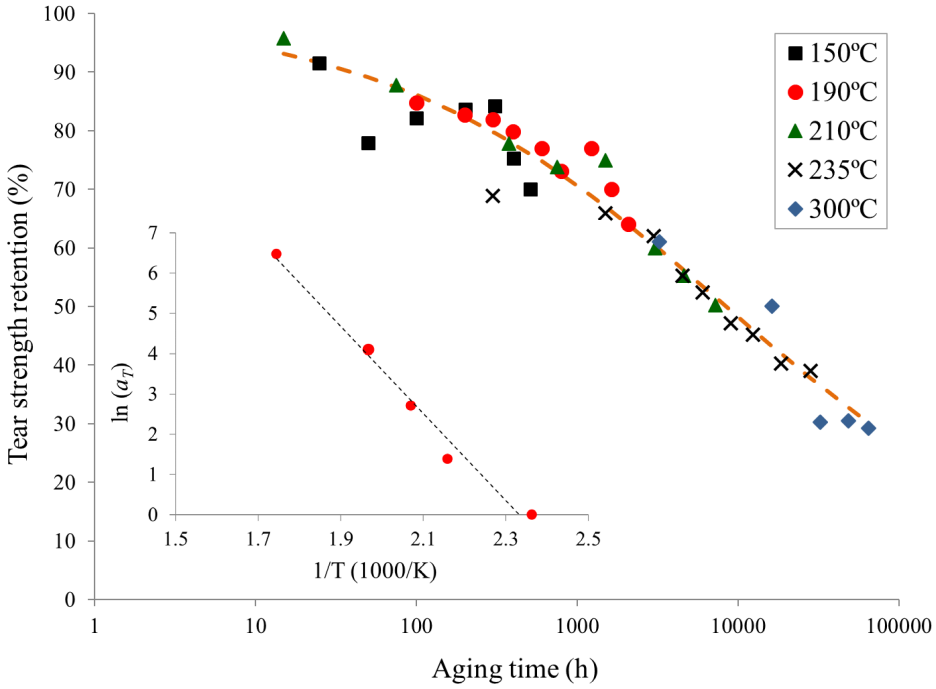

Figure 11. TTS master curve at a temperature of 150°C with fit by Hill equation for Fabric # 2 (In insert: Arrhenius plot of the shift factors).

The fit of the master curve at 150°C with the Hill equation is also shown in Figure 11. The values of the slope and the inflexion point are 0.41 and 8455 h respectively. These values are much lower for the slope and higher for the inflexion point compared to what was obtained for Fabric #1, which is coherent with the better thermal aging performance reported for Fabric #2. The value of the lower asymptote corresponding to the ultimate tear strength could not be obtained with enough precision due to the lack of data points in the lower range of the sigmoid curve.

As for Fabric #1, no change in the FTIR spectrum was observed for Fabric #2 as a result of thermal aging. Figure 12 provides SEM images of an unaged specimen and a specimen aged for 100 hours at 300°C. No difference in the fiber microstructure between the unaged and aged condition could be observed either.

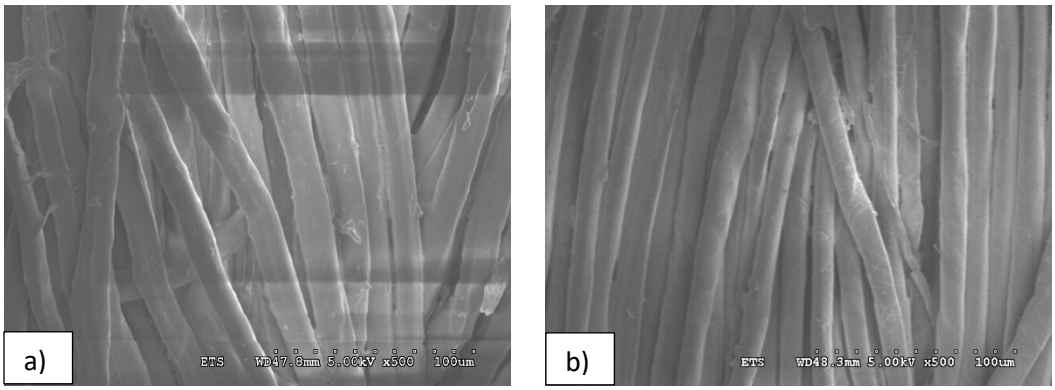

Figure 12. SEM pictures of Fabric # 2, a) unaged and b) aged at 300°C for 100 hours (magnification x 500).

4.3 Fabric #3

Figure 13 shows the TGA of Fabric #3. As this fabric is also a blend of Kevlar® and Nomex®, the thermal degradation pattern is similar to what has been observed with Fabric #2. However, the Kevlar® content in Fabric #3 is much higher than that of Nomex®. As a result, the main weight drop is in the 530-700°C range associated with the degradation of Kevlar®.

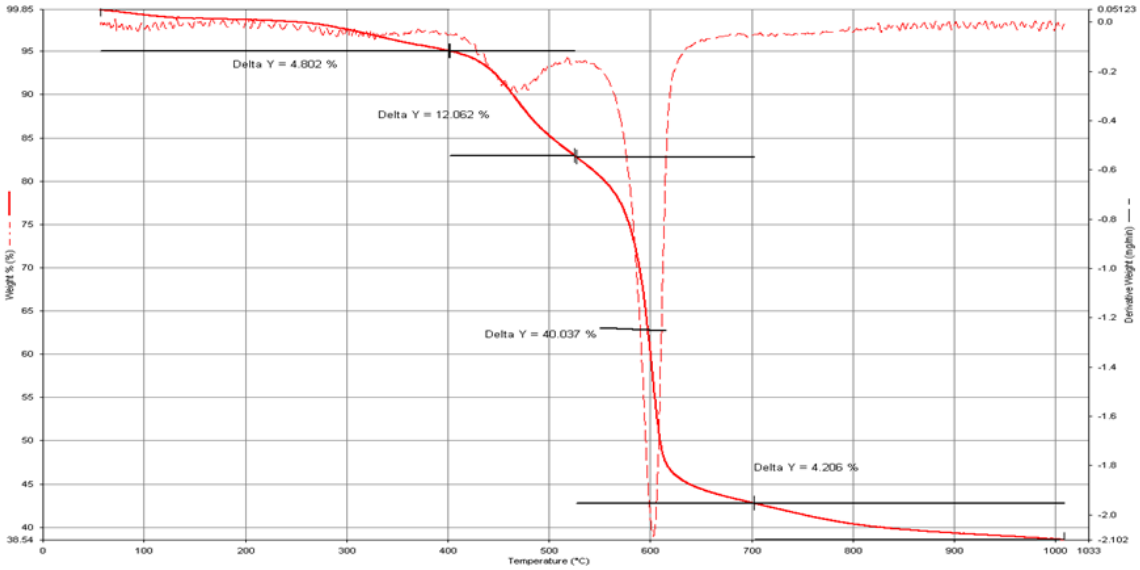

Figure 13. TGA and time derivative spectrum of Fabric #3.

The tear retention of Fabric #3 (Figure 14) was also better than that of Fabric #1. The tear strength retention at 150°C was 85% even after 500 hrs of exposure.

The TTS master curve using the data at 150°C as reference is shown in Figure 15. The Arrhenius plot created using the shift factors from the TTS technique is provided as an insert in Figure 15.

The correlation coefficient for the Arrhenius plot is 0.988, which indicates an excellent agreement with the model. The activation energy calculated using this approach is 113 kJ/mol. This value is higher than that obtained for Fabric #1 and #2.

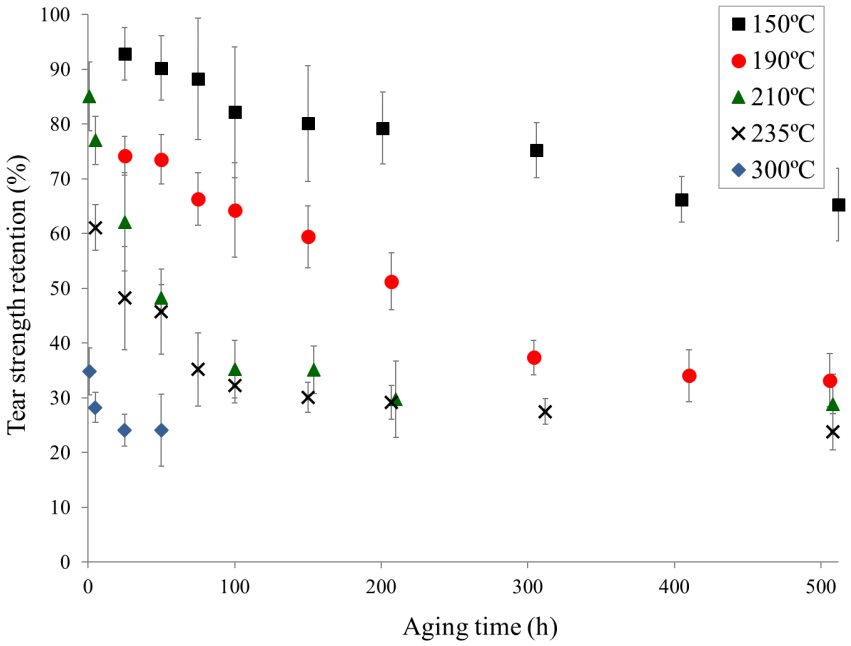

Figure 14. Variation of the tear strength retention as a function of the aging time at aging temperatures of 150, 190, 210, 235, and 300°C for Fabric # 3.

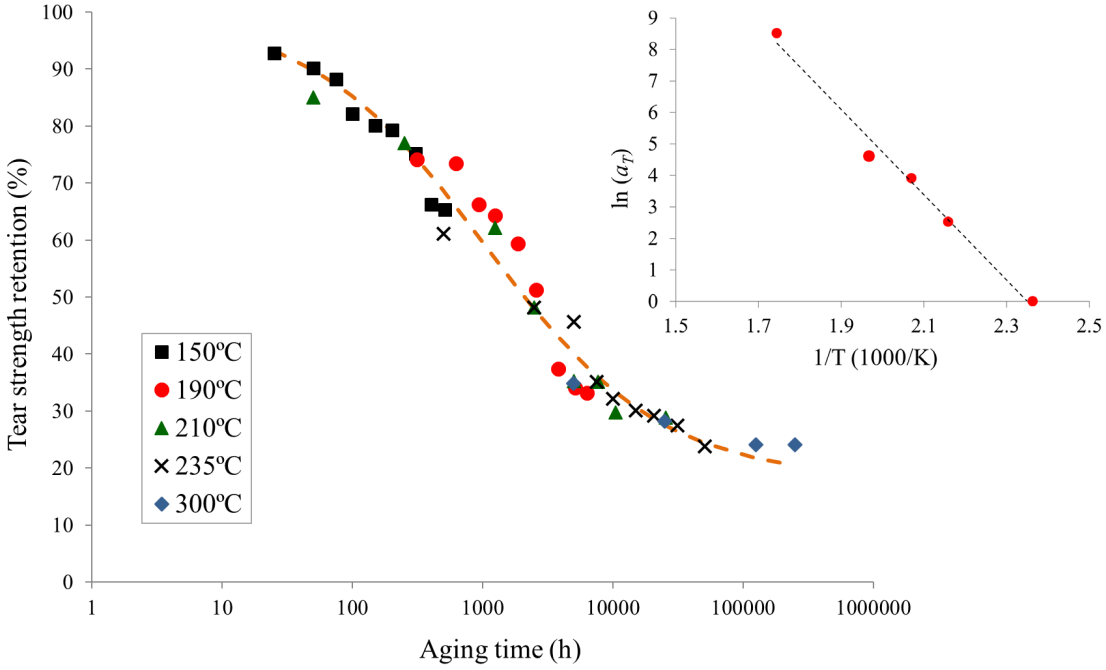

Figure 15. TTS master curve at a temperature of 150°C with fit by Hill equation for Fabric # 3 (In insert: Arrhenius plot of the shift factors).

The fit of the master curve at 150°C with the Hill equation is also shown in Figure 15. The value of the slope is 0.64, which is similar to what was obtained for Fabric #1. The value of the inflexion point is 1050 h. It is situated between that of Fabric #1 and Fabric #2. The value for the lower asymptote corresponding to the ultimate tear strength retention is 18%.

Similarly to Fabric #1 and #2, no difference in the FTIR spectrum and fiber morphology was noted as a result of thermal aging.

4.4 Fabric #4

Figure 16 shows the TGA curve for Fabric #4, which is a blend of Kevlar®, Nomex®, and PBO. The weight loss took place in several steps. The weight loss below 410°C may be due the decomposition of materials used as a finish on the fabric as well as the release of adsorbed water. The major weight loss occurring at 580°C is associated with the decomposition of Kevlar® and the smaller drop in weight between 410 and 520°C to the decomposition of Nomex®. The weight loss between 650 and 800°C is attributed to the degradation of PBO in agreement with the literature[5]. Its degradation temperature is higher than that of Kevlar® and Nomex® due to the heterocyclic rigid conformation of the molecules and the stability of the C-O linkage in the heterocyclic rings in the backbone.

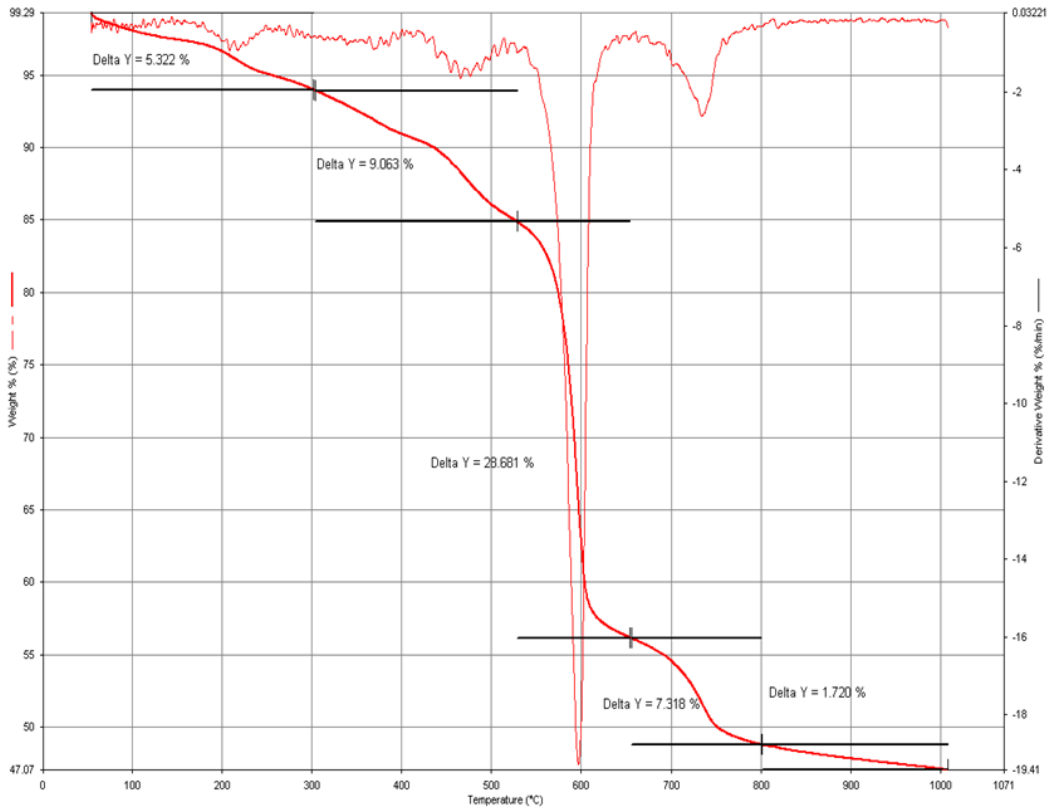

Figure 16. TGA and time derivative spectrum of Fabric #4.

The tear strength retention of Fabric #4 is shown in Fig. 17. The fabric lost 25% of its strength after 25 hours at 150°C and more than 80% after 5 hours at 300°C.

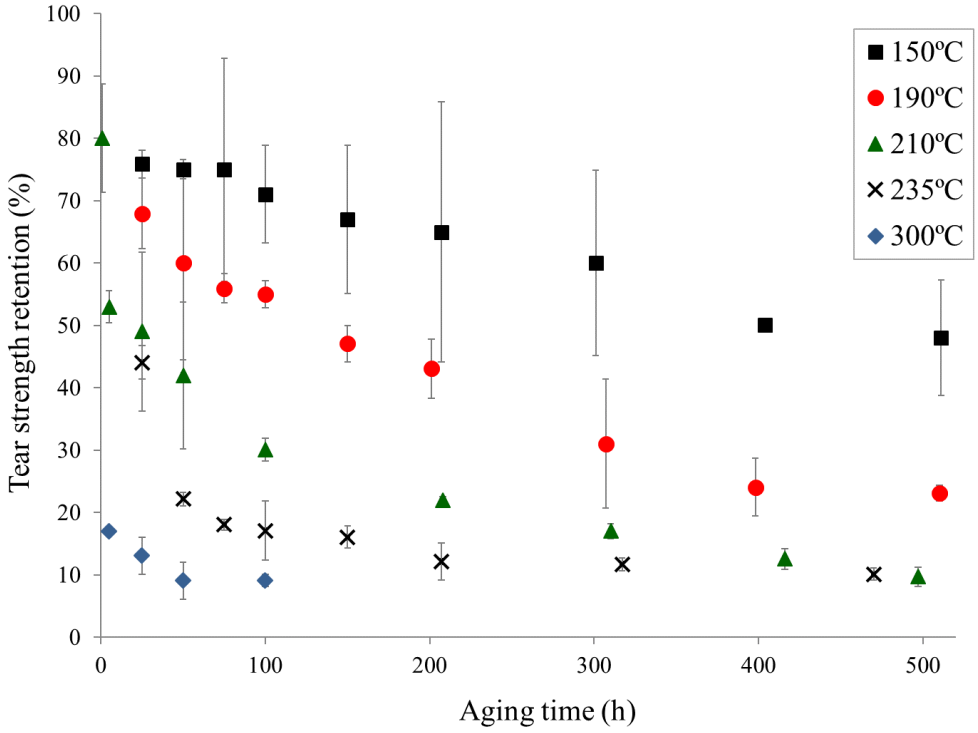

Figure 17. Variation of the tear strength retention as a function of the aging time at aging temperatures of 150, 190, 210, 235, and 300°C for Fabric # 4.

The TTS master curve using the data at 150°C as reference is shown in Figure 18. The Arrhenius plot created using the shift factors from the TTS technique is shown as an insert in Figure 18. The Arrhenius model accommodates the data satisfactorily with a correlation coefficient of 0.986. The activation energy is 103 kJ/mol. This value is situated in between what was obtained for Fabric #2 and Fabric #3.

The fit of the master curve at 150°C with the Hill equation is also shown in Figure 18. The value of the slope is 0.51, which is also in between what was obtained for Fabric #2 and Fabric #3. On the other hand, the inflexion point is at 550 hours, which is much lower than the values for Fabric #2 and #3. The value of the tear strength retention at the lower asymptote is 2%.

Similarly to the other fabrics studied, no difference in the FTIR spectrum and fiber morphology was noted as a result of thermal aging.

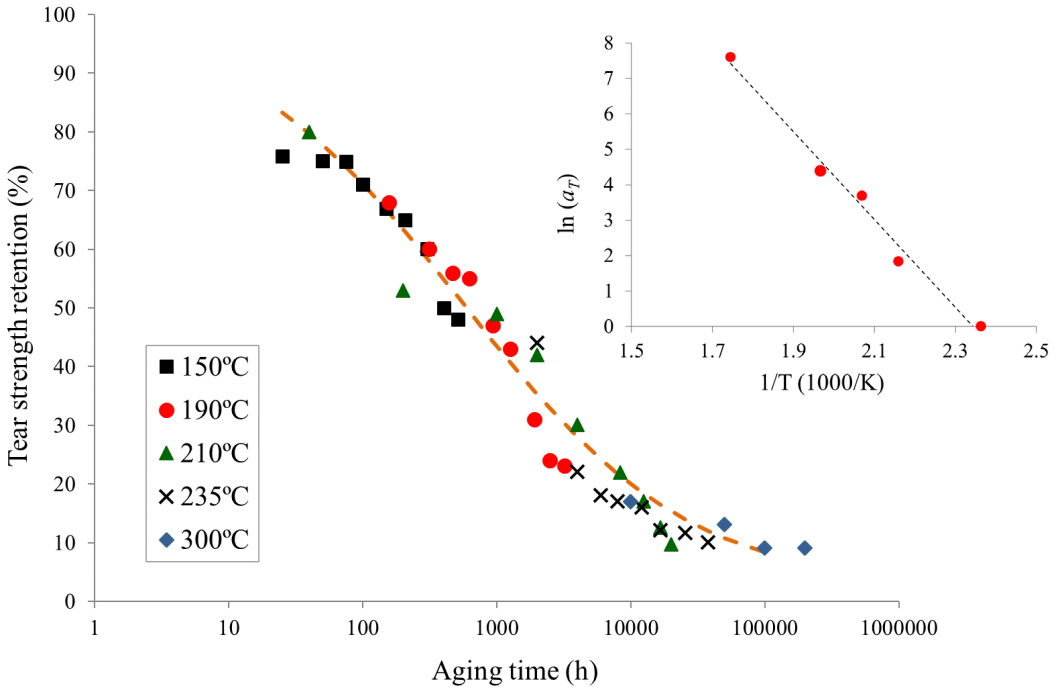

Figure 18. TTS master curve at a temperature of 150°C with fit by Hill equation for Fabric # 4 (In insert: Arrhenius plot of the shift factors).

4.5 Fabric #5

Figure 19 displays the TGA curves for Fabric #5, which contains Kevlar® and Basofil®. The weight loss took place in two steps. The initial weight loss between 300 and 500°C is associated to the decomposition of melamine in agreement with the decomposition temperature of 400°C in inert atmosphere reported in the litterature[5]. Melamine is known to evaporate when decomposing, thus acting as a heat sink in fire situations[37]. The second weight loss between 530 and 650°C is attributed to the degradation of Kevlar®.

The tear retention of Fabric #5 (Fig. 20) also displayed a decrease in tear strength retention after aging. However, the sample retained 85% of its strength at 150°C even after 500 hours of exposure. At 300°C, the strength retention was 50% after 1 hour of exposure and 25% after 5 hours.

The TTS master curve using the data at 150°C as reference is shown in Figure 21. The Arrhenius plot created using the shift factors from the TTS technique is displayed as an insert in Figure 21. The agreement with the Arrhenius model is excellent with a correlation coefficient of 0.999. The activation energy calculated using this approach is 105 kJ/mol. This value is similar to what has been obtained for Fabric #4.

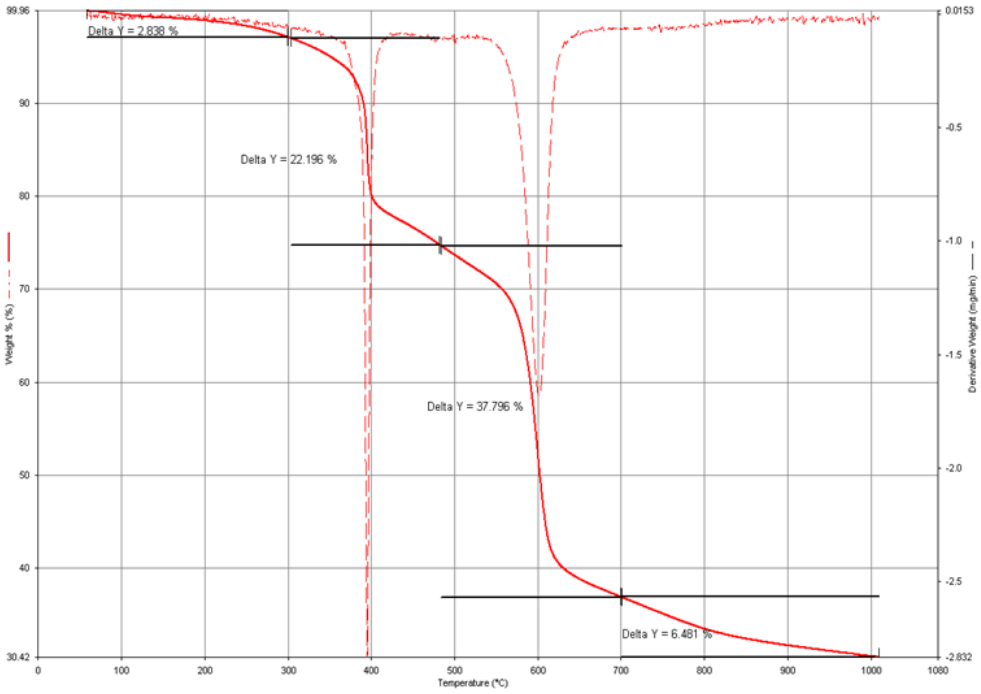

Figure 19. TGA and time derivative spectrum of Fabric #5.

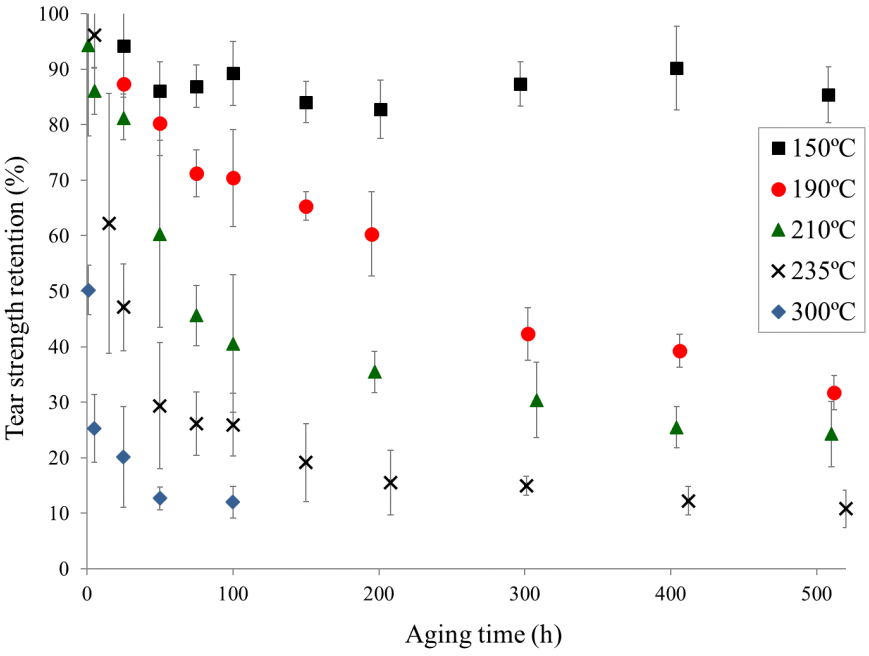

Figure 20. Variation of the tear strength retention as a function of the aging time at aging temperatures of 150, 190, 210, 235, and 300°C for Fabric # 5.

The fit of the master curve at 150°C with the Hill equation is also shown in Figure 21. The value of the slope is 0.88, much higher to what has been obtained for the other fabrics so far. The

inflexion point is at 3092 hours, which is the second highest value obtained so far. The value of the tear strength retention at the lower asymptote is 8%.

Similarly to the other fabrics studied, no difference in the FTIR spectrum and fiber morphology was noted as a result of thermal aging.

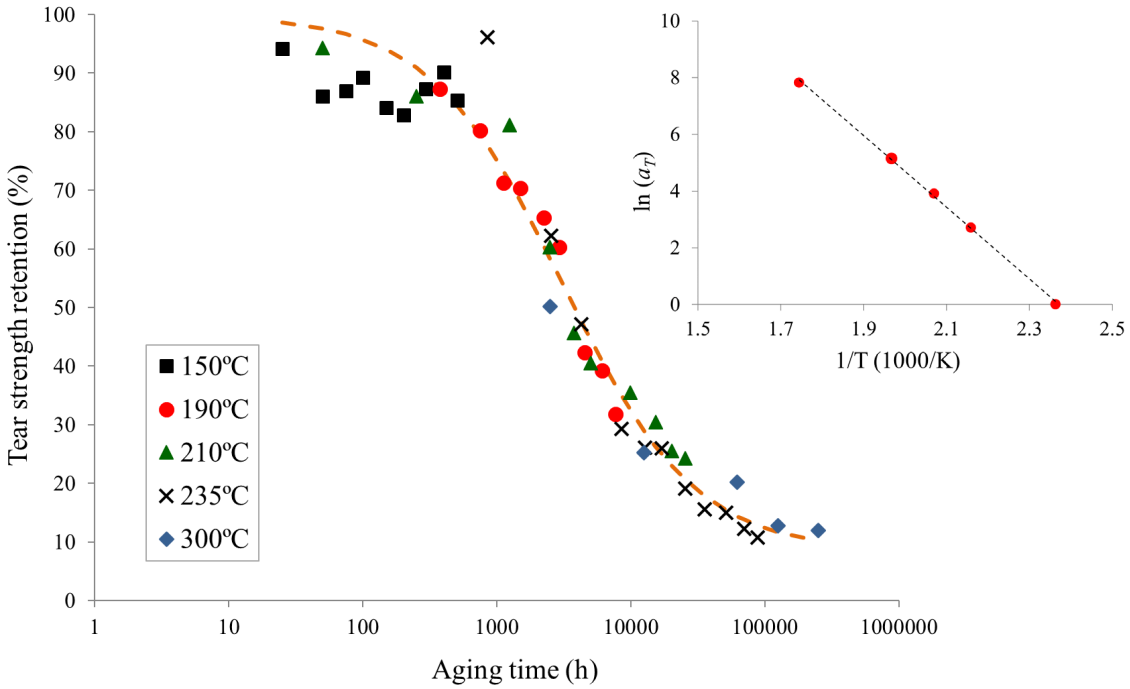

Figure 21. TTS master curve at a temperature of 150°C with fit by Hill equation for Fabric # 5 (In insert: Arrhenius plot of the shift factors).

4.6. Fabric #6

The variation of the tear strength retention of Fabric #6, which only contains Nomex®, is shown in Figure 22. The fabric maintained 80% of its tear strength at 150°C for the longest exposure times. At 300°C, the loss in tear strength was 25% after 1 hour and 37% after 5 hours.

The data analyzed using the TTS technique are shown in Figure 23. The Arrhenius plot created using the shift factors to form the master curve using the data at 150°C as reference is displayed as an insert in Figure 23. The agreement with the Arrhenius model is good with a correlation coefficient of 0.96. The activation energy calculated using this approach is 81 kJ/mol. This is the lowest value of activation energy obtained so far.

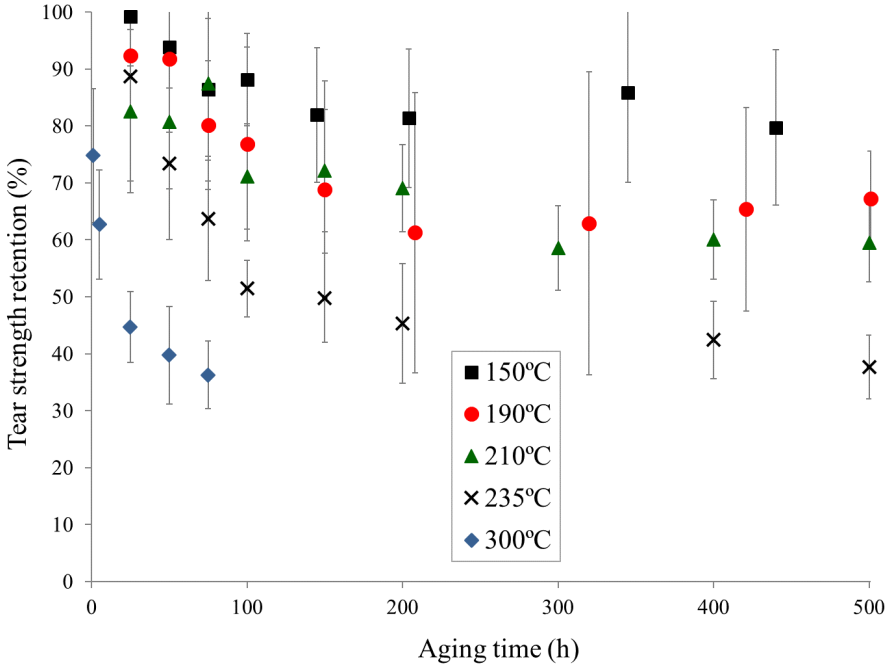

Figure 22. Variation of the tear strength retention as a function of the aging time at aging temperatures of 150, 190, 210, 235, and 300°C for Fabric # 6.

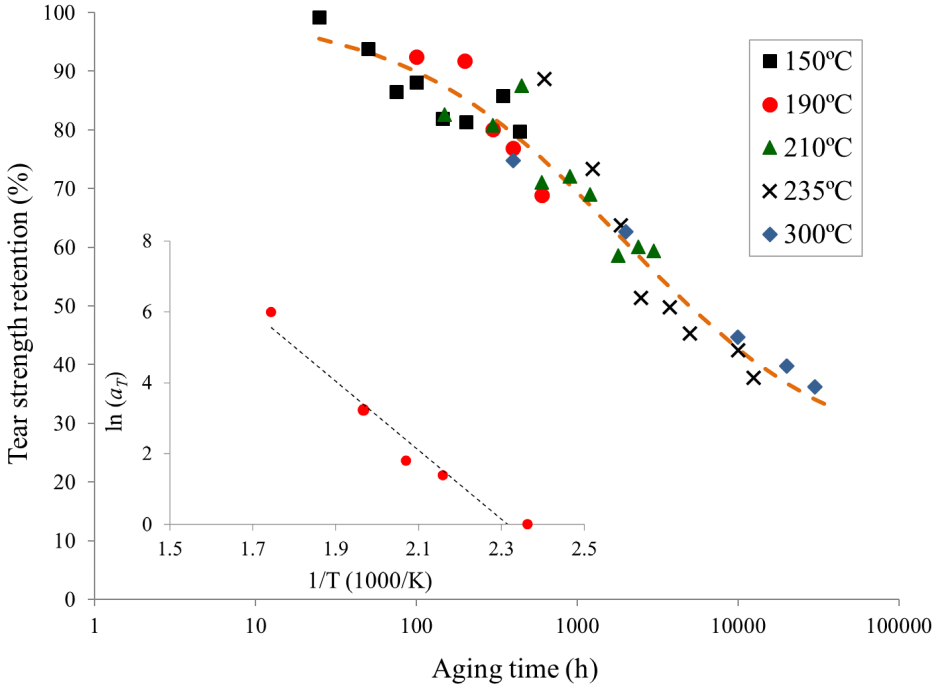

Figure 23. TTS master curve at a temperature of 150°C with fit by Hill equation for Fabric # 6 (In insert: Arrhenius plot of the shift factors).

The fit of the master curve at 150°C with the Hill equation is also shown in Figure 23. The value of the slope is 0.65, which is similar to what was obtained for Fabric #1 and #3. The inflexion point is at 1895 hours. The value of the tear strength retention at the lower asymptote is in the range of 23% but the insufficient number of data points in the lower range of the sigmoid curve made that determination quite imprecise.

Similarly to the other fabrics studied, no difference in the FTIR spectrum and fiber morphology was noted as a result of thermal aging.

4.7 Fabric #7

Data regarding the thermal decomposition of Fabric #7, which contains Kevlar® and PBI, have been published by Arrieta et al.[17]. One main thermal event at 580°C can be observed in the differential thermal analysis curve. It can be attributed to the decomposition of Kevlar®. The decomposition temperature of PBI in nitrogen has been reported to be over 1,000°C[5].

The variation of the tear strength retention of Fabric #7 is shown in Figure 24. The fabric maintained 70% of its tear strength after 550 hours at 150°C. At 300°C, the loss in tear strength was 25% after 1 hour and 50% after 5 hours.

The data analyzed using the TTS technique are shown in Figure 25. The Arrhenius plot created using the shift factors to form the master curve using the data at 150°C as reference is displayed as an insert in Figure 25. The agreement with the Arrhenius model is excellent with a correlation coefficient of 0.998. The activation energy is 111 kJ/mol, which is almost as high as what has been obtained for Fabric #3.

The fit of the master curve at 150°C with the Hill equation is also shown in Figure 25. The value of the slope is 0.95, which is the highest value recorded. The inflexion point is at 688 hours, which is in the same range as Fabric #4. The value of the tear strength retention at the lower asymptote is 17%, similar to what was obtained for Fabric #3.

Similarly to the other fabrics studied, no difference in the FTIR spectrum and fiber morphology was noted as a result of thermal aging.

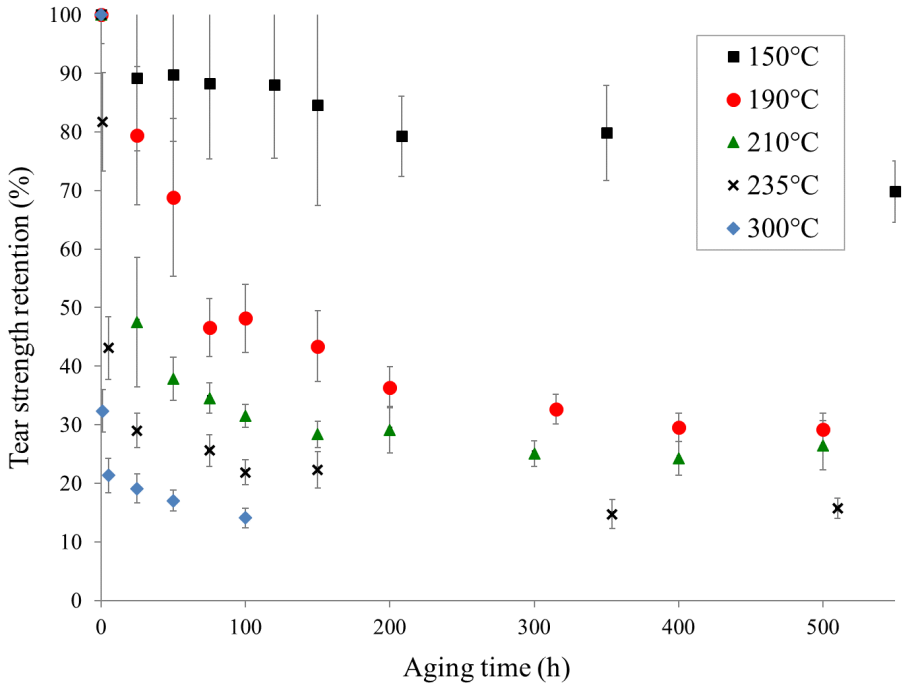

Figure 24. Variation of the tear strength retention as a function of the aging time at aging temperatures of 150, 190, 210, 235, and 300°C for Fabric # 7.

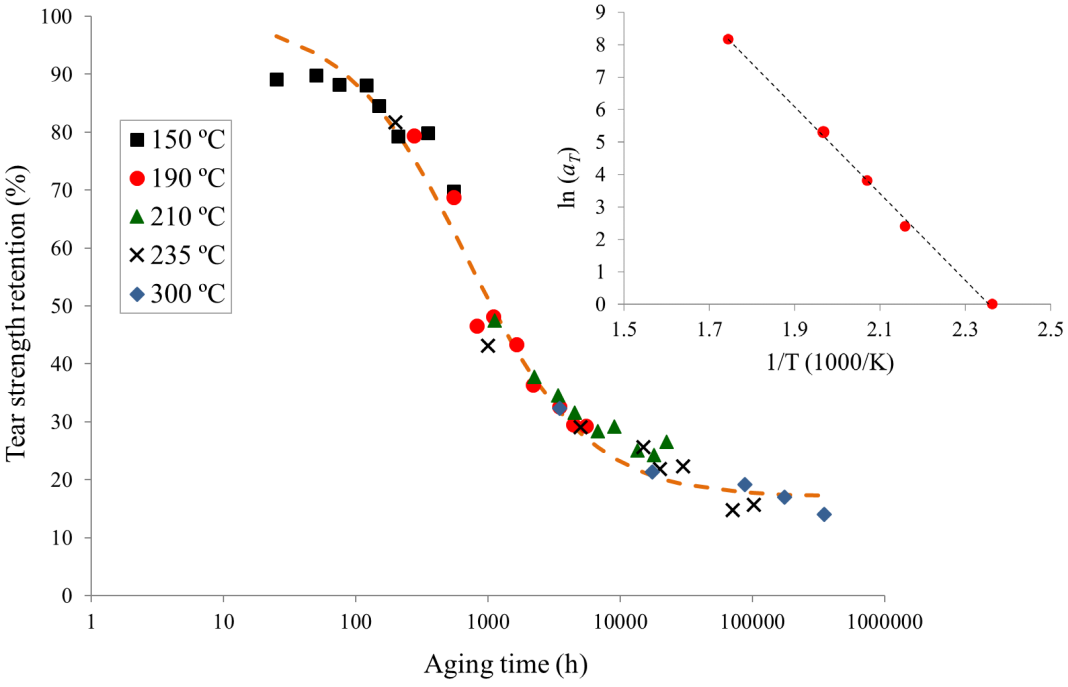

Figure 25. TTS master curve at a temperature of 150°C with fit by Hill equation for Fabric # 7 (In insert: Arrhenius plot of the shift factors).

5. Discussion

Results obtained with all seven fabrics studied showed a significant decrease in tear strength as aging time and temperature increased. These observations are in agreement with what has been reported in the literature for the different fibers constitutive of the fabrics. For instance, a 50% reduction in tensile strength of a 60/40 wt% Kevlar®/PBI spun yarn was recorded after 300 hours of exposure at 190°C[16]: the loss in tensile strength rose to 60% when the exposure time was increased to 400 hours at the same aging temperature of 190°C, and to 75% with an aging temperature of 220°C for the same 300h exposure time. In the case of Nomex® fibers, 160 hours of aging at 300° led to a 30% reduction in tensile strength[18]. The exposure time to reach the same 30% reduction in tensile strength was only 15 hours at 350°C.

These reductions in the fabric tear strength with thermal aging may be attributed to modifications in the chemical and crystalline structure of the constitutive fibers. For instance, a disruption of the crystalline lattice in the direction perpendicular to the coplanar sheets with a simultaneous increase in the crystallite size in the parallel direction were reported for Kevlar® as a result of thermal aging[17]. Nomex® fibers held at 200°C showed a gradual decrease in crystallinity with increasing exposure time[18]. They reached a state of zero crystallinity after 1750h of exposure. In the case of PBI, a reduction of the glass transition temperature as a result of thermal aging pointed towards random chain scissions[17].

Figure 26 shows a comparison of the Hill equation fits for all seven fabrics tested. The results are expressed in terms of tearing force. For Fabric # 1, the initial tearing force was very high but dropped quite rapidly and eventually reached a zero value after long-term thermal aging. Fabric # 4 started with about the same strength as Fabric # 1 but lost it more slowly. On the other hand, Fabric # 7 started with a slightly lower tearing force value; however, it degraded at a slower pace than Fabric # 1 and more importantly kept a higher level of ultimate residual strength. The last group of fabrics (Fabric #2, #3, #5, and #6) displayed a much lower initial tearing force and a relatively similar degradation behavior over time. The difference in structure between the fabrics (see Table 2) is not expected to affect the thermal aging results when the data are expressing in terms of performance retention. Indeed, a comparison between a Kevlar/PBI fabric, Kevlar/PBI yarns, and Kevlar threads showed that the response of the fabric to thermal aging was controlled by the constitutive yarn aging behavior and that the fabric structure had a limited effect[16].

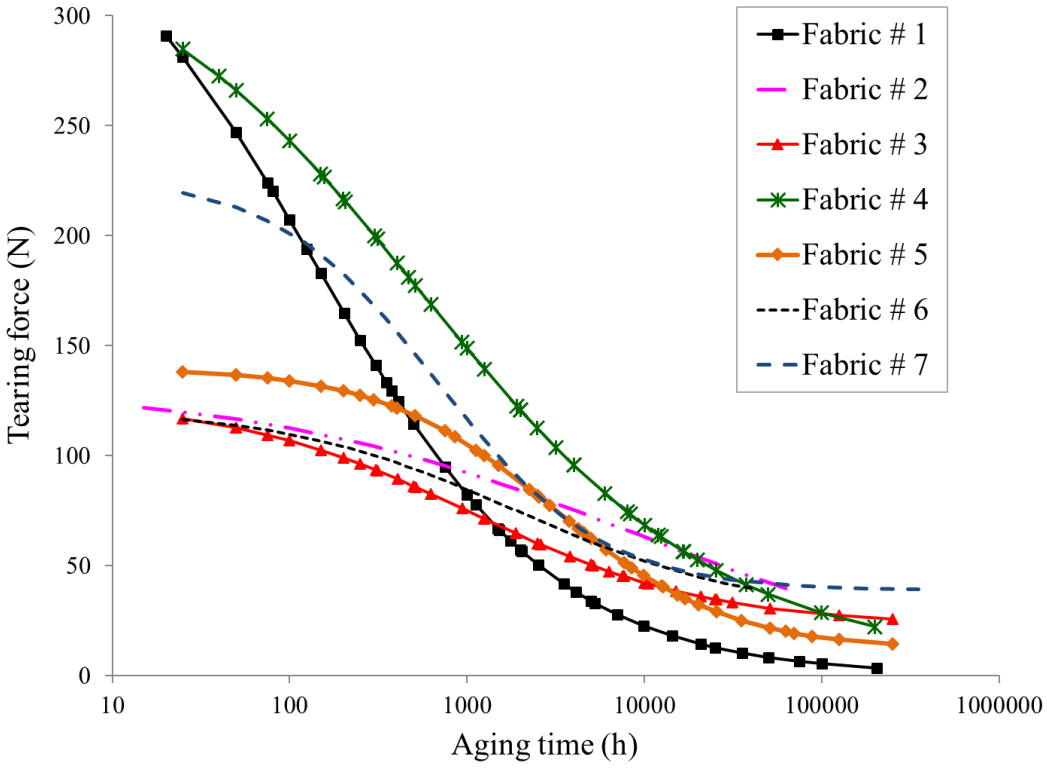

Figure 26. Hill equation fits of the tearing force data shifted on a master curve at a temperature of 150°C for all the fabrics tested.

The values of the parameters provided by the fit of the data by the Arrhenius and Hill equation for each fabric are provided in Table 3. The value of the lower asymptote α in the Hill equation has been converted to ultimate residual tearing force for increased meaningfulness. The value of initial tearing force of each fabric is also given in Table 3. The characteristics that would be ideal for a fabric designed for long-term fire protection are:

- A high value of initial strength to compensate for the unavoidable losses occurring over time;
- A high value of the activation energy so that the effect of a temperature increase is limited;
- A low value of the Hill equation slope so that the decrease in strength over time takes place at a slow rate;
- A high value of the Hill equation inflexion point to retard as much as possible the degradation; and
- A high value of ultimate residual strength to have the fabric always maintain some level of physical integrity.

However, none of the fabrics studied appears to stand as displaying all these characteristics. The best solution is thus a compromise that will depend on the type of activity conducted and the

type of conditions experienced. More research is needed to define the value of each parameter in both model equations that would correspond to the minimum level depending on the conditions experienced.

Table 3. Values provided by the fitting of the thermal aging data with the Arrhenius model and the Hill equation along with the initial tearing force (*: imprecise value resulting from the lack of data in the long time range).

Fabric	Initial tearing force (N)	Activation energy Ea (kJ/mol)	Hill equation inflexion point K (h)	Hill equation slope n	Ultimate residual tearing force (N)
# 1	374 ± 4	95 ± 6	140	0.64	0
# 2	131 ± 5	90 ± 7	8422	0.41	*
# 3	125 ± 5	113 ± 7	1050	0.64	23
# 4	342 ± 1	103 ± 7	550	0.51	7
# 5	140 ± 4	105 ± 2	3092	0.88	12
# 6	122 ± 8	81 ± 9	1895	0.65	28*
# 7	227 ± 11	111 ± 3	688	0.95	39

Using the data displayed in Table 3, a preliminary analysis was performed to look for eventual correlations between the fabric composition, more specifically its Kevlar® content, and its thermal aging behavior. Figure 27 shows the variation of the activation energy with the Kevlar® content. Even if more data points would be needed to confirm this trend, the activation energy seems to be higher when Kevlar® is blended with other fibers, either Nomex® IIIA (see Table 1 for detail of composition), Basofil®, PBI, or a blend of Nomex® and PBO. On the other hand, the activation energy is lower when the fabric only contains Kevlar® or Nomex® (or Nomex® IIIA). This might be associated with the fact that in many instances, blending different materials creates synergistic effects allowing them to reach higher performances[38]. In the case of the Hill equation parameters, no clear trend could be identified at this point.

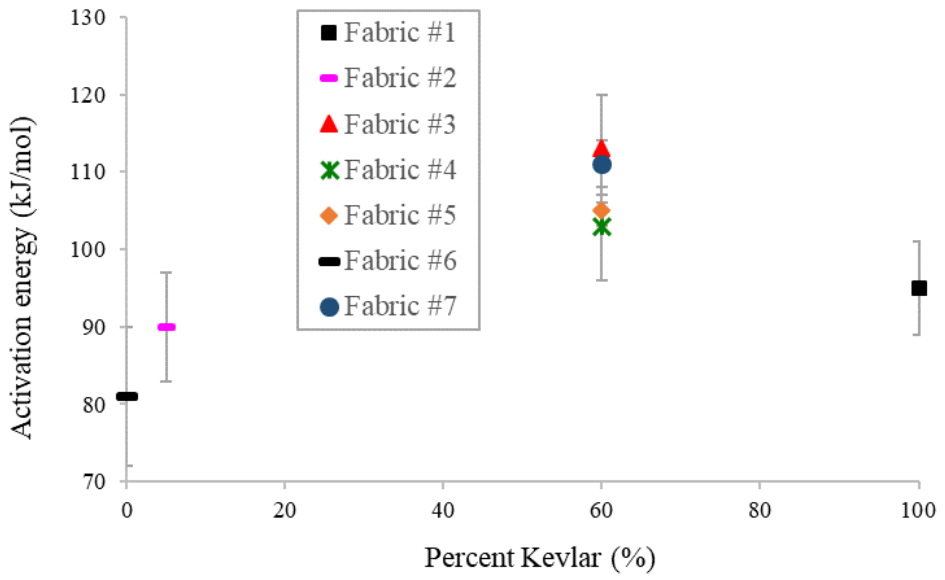

Figure 27. Variation of the activation energy as a function of Kevlar® content.

In terms of aging mechanism, the qualitative analysis of the fabric FTIR spectra showed no evidence of chemical changes between the aged and unaged samples. No difference was observed by SEM either. A similar absence of effect by FTIR had also been reported by Arrieta et al. for a Kevlar-PBI fabric exposed to thermal aging at temperatures between 190 and 320°C[16]. This absence of degradation signature on the FTIR spectra and SEM pictures of the fabrics despite the large loss in tear strength observed could be attributed to the much larger sensitivity of mechanical properties, in particular at failure, to polymer degradation resulting from thermal aging[39]. In addition, a change in crystallinity as a result of thermal aging has been reported for several of the fibers used in the fabrics studied here and may explain in part the large loss in tear strength observed. For instance, in the case of Kevlar®, an increase in the crystallite size in the direction parallel to the coplanar sheets was observed to occur simultaneously with a disruption of the crystalline lattice in the perpendicular direction[17]. The thermal aging of Nomex® fibers also induced a gradual decrease in crystallinity with aging time[18]. For melamine fibers, thermal aging generated an increase in crystallinity accompanied with a change in the crystalline structure and an increase in the crystallite size[19].

5. Conclusions

A data analysis method was developed to allow comparing in a quantitative manner the effect of thermal aging on the mechanical performance of fire protective fabrics. It consists in a system of two equations fitting the time-temperature-performance data: the Arrhenius model combined with the time-temperature superposition principle that informs about the influence

of the aging temperature, and the 3-parameter Hill equation that describes the effect of time on the aging process.

This data analysis method was used to analyze and compare the effect of thermal aging at temperatures between 150 and 300°C for up to 500h on the tear strength of seven fire protective fabrics made with different ratios of various high-performance fibers. A significant level of decrease in tear strength was observed for all fabrics even at a temperature as low as 150°C: depending on the fabric, the loss in tear strength ranged between 15 and 33% after 150h of aging at 150°C, a temperature much lower than the thermal index of the fibers constituting these fabrics.

A very good agreement was observed for all the fabrics when the Arrhenius model was used to describe the TTS shift factors. When the activation energy obtained for the different fabrics was expressed as a function of the Kevlar® content in these fabrics, a higher value could eventually be seen when the Kevlar® fibers were blended with other fibers. On the other hand, the activation energy appears to be lower when the fabric only contains Kevlar® or Nomex® (or Nomex® IIIA).

The master curves provided by the TTS principle for the different fabrics were described satisfactorily by the Hill equation. For some fabrics, the initial tearing force was very high but dropped quite rapidly as a result of thermal aging and eventually reached a zero value after long-term thermal aging. Other fabrics started with a slightly lower tearing force value, degraded at a slower pace, and kept a non-null level of ultimate residual force. Others displayed a much lower initial tearing force and a relatively similar degradation behavior over time.

This method provides a means to quantitatively compare the effect of thermal aging on the performance of different fabrics, and more specifically distinguish the individual contribution of the aging temperature and time. With further work, it could also provide a tool for the optimization of the composition of fabrics based on the conditions they would experience in service.

Acknowledgements

This work was conducted while the authors were working at École de technologie supérieure (Montréal, QC, Canada). They would like to thank Innotex and PGI Difco for graciously providing the fabrics, Dr. Carlos Arrieta for helping with the data analysis as well as MITACS and CTT Group for financial support.

References

1. Fahy, R. F.; LeBlanc, P. R.; Molis, J. L. *Firefighter Fatalities in the United States - 2016*; NFPA: Quincy, MA, **2017**.

2. Haynes, H. J. G.; Molis, J. L. *U.S. Firefighter Injuries - 2015*; NFPA: Quincy, MA, **2016**.

3. Matt, S. E., Shupp, J. W., Carter, E. A., Flanagan, K. E. and Jordan, M. H. *Journal of Burn Care & Research* **2012**, *33*, 147-151.

4. Chang, K. K. In *ASM Handbook*, ASM International: Russell Township, OH, **2001**; Vol. 21, pp 41 - 45.

5. Bourbigot, S. and Flambard, X. *Fire and Materials* **2002**, *26*, 155-168.

6. Cyr, A. *The Guide to Textile Fibers: Clothing and Fashion Industry*, 2nd Edition. **2016**. CreateSpace Independent Publishing Platform.

7. Horrocks, A. R., Eichhorn, H., Schwaenke, H., Saville, N., Thomas, C. In *High Performance Fibres*. Woodhead Publishing Limited: Cambridge, UK, **2001**, 281-324.

8. Chae, H. G. and Kumar, S. *J. Appl. Polym. Sci.* **2006**, *100*, 791-802.

9. Vogelpohl, T. L. Post-Use Evaluation of Fire Fighter's Turnout Coats. Master's Thesis, University of Kentucky, Lexington, KY, 1996.

10. Cotterill, D. Post Use Evaluation of Firefighter Turnout Gear. Master's Thesis, University of Kentucky, Lexington, KY, 2009.

11. Trenkamp, S. L. Post Use Analysis of Firefighter Turnout Gear Phase II. Master's Thesis, University of Kentucky, Lexington, KY, 2011.

12. Cinnamon, M. L. Post Use Analysis of Firefighter Turnout Gear - Phase III. Master's Thesis, University of Kentucky, Lexington, KY, 2013.

13. McQuerry, M., Klausing, S., Cotterill, D. and Easter, E. *Fire Technology* **2015**, *51*, 1149-1166.

14. Hart, S. V. *Third Status Report to the Attorney General on Body Armor Safety Initiative Testing and Activities*; National Institute of Justice: Washington, D.C., **2005**.

15. Fulton M., Rezazadeh M. & Torvi D. In Advanced characterization and testing of textiles. Elsevier: Duxford, UK, 2017, 93-125.

16. Arrieta, C., David, E., Dolez, P. and Toan, V.-K. *J. Appl. Polym. Sci.* **2010**, *115*, 3031-3039.

17. Arrieta, C., David, E., Dolez, P.; and Vu-Khanh, T. *Polym. Compos.* **2011**, *32*, 362-367.

18. Jain, A. and Vijayan, K. *Bulletin of Materials Science* **2002**, *25*, 341-346.

19. Rajeev, R. S., De, S. K., Bhowmick, A. K., Gong, B. and Bandyopadhyay, S. *Journal of Adhesion Science and Technology* **2002**, *16*, 1957-78.

20. Wu, Z., Li, F., Huang, L., Shi, Y., Jin, X., Fang, S., Chuang, K., Lyon, R. E., Harris, F. W. and Cheng, S. Z. D. *Journal of Thermal Analysis and Calorimetry* **2000**, *59*, 361-373.

21. Ozgen, B. and Pamuk, G. *Industria Textila* **2014**, *65*, 254-262.

22. Rossi, R. M., Bolli, W. and Stampfli, R. *International Journal of Occupational Safety and Ergonomics* **2008**, *14*, 55-60.

23. Hoschke, B. N. *Fire Safety Journal* **1981**, 4, 125-137.

24. El Aidani, R., Dolez, P. I. and Vu-Khanh, T. *J. Appl. Polym. Sci.* **2011**, *121*, 3101-3110.

25. Verdu, J. In *Techniques De L'ingénieur: Traité Plastiques et Composites*, Techniques de l'Ingénieur: Paris, France, **2002**; Vol. AM3152.

26. Gillen, K. T., Celina, M., Clough, R. L. and Wise, J. *Trends in Polymer Science* **1997**, *5*, 250-257.

27. Crine, J. P. *IEEE Transactions on Electrical Insulation* **1991**, *26*, 811-818.

28. Christopoulos, A. and Lew, M. J. *Crit. Rev. Biochem. Mol. Biol.* **2000**, *35*, 359-391.

29. Goutelle, S., Maurin, M., Rougier, F., Barbaut, X., Bourguignon, L., Ducher, M. and Maire, P. *Fundam. Clin. Pharmacol.* **2008**, *22*, 633-648.

30. Lombardo, T., Chabas, A., Lefèvre, R.-A. and Ionescu, A. *Glass Technology* **2005**, *46*, 192-196.

31. Triki, E., Arrieta, C., Boukehili, H. and Vu-Khanh, T. *Polym. Compos*. **2012**, *33*, 1007-1017

32. Marta, E., Mosquera, G., Jamond, M., Alonso, A. M., Tasco J. M. D. *Chem. Mater* **1994**, 6, 1918-1924.

33. Shubha, M., Parimala, H. V., Vijayan, K. *J. Mater. Sci. Lett.* **1993**, *12(1)*, 60-2.

34. Villar-Rodil, S., Martinez-Alonso, A., Tascon, J. M. D. *J. Anal. Appl. Pyrolysis*. **2001**, 58-59, 105-115.

35. Innotex Fabrics. 2016. Accessed July 20, 2018. http://innotexprotection.com/wp-content/uploads/2017/07/fabrics-en.pdf

36. Guide for the Selection and Use of Flame Resistant Workwear. 2014. Canadian Association of Petroleum Producers (CAPP). Accessed July 20, 2018. www.capp.ca/~/media/capp/customer-portal/publications/258938.pdf

37. Levchik, S., Balabanovich, A., Levchik, G., Costa, L. *Fire and Materials*. **1997**, 21(2), 75-83.

38. Miao M. In Engineering of High-Performance Textiles. Elsevier: Duxford, UK, **2018**, 59-79.

39. Verdu J. *Vieillissement des plastiques*. **1984**. Association française de normalisation.